

Y. Corre, J-L. Gardarein, J. Gaspar, F. Rigollet, G. Arnoux, S. Devaux, T. Eich,
C. Giroud, F. Marcotte, B. Sieglin and JET EFDA contributors

Heat Flux Calculation Using Embedded Thermocouple in W-Coated CFC Tiles in the JET Tokamak

“This document is intended for publication in the open literature. It is made available on the understanding that it may not be further circulated and extracts or references may not be published prior to publication of the original when applicable, or without the consent of the Publications Officer, EFDA, Culham Science Centre, Abingdon, Oxon, OX14 3DB, UK.”

“Enquiries about Copyright and reproduction should be addressed to the Publications Officer, EFDA, Culham Science Centre, Abingdon, Oxon, OX14 3DB, UK.”

The contents of this preprint and all other JET EFDA Preprints and Conference Papers are available to view online free at www.iop.org/Jet. This site has full search facilities and e-mail alert options. The diagrams contained within the PDFs on this site are hyperlinked from the year 1996 onwards.

Heat Flux Calculation Using Embedded Thermocouple in W-Coated CFC Tiles in the JET Tokamak

Y. Corre¹, J-L. Gardarein², J. Gaspar², F. Rigollet², G. Arnoux³, S. Devaux⁴,
T. Eich⁴, C. Giroud³, F. Marcotte³, B. Sieglin⁴
and JET EFDA contributors*

JET-EFDA, Culham Science Centre, OX14 3DB, Abingdon, UK

¹*CEA, IRFM, F-13108 Saint-Paul-lez-Durance, France.*

²*Aix-Marseille University, IUSTI UMR 7343, 13013 Marseille, France*

³*EURATOM-CCFE Fusion Association, Culham Science Centre, OX14 3DB, Abingdon, OXON, UK*

⁴*Max-Planck-Institut für Plasmaphysik, EURATOM-Assoziation, Garching, Germany*

** See annex of F. Romanelli et al, "Overview of JET Results",
(23rd IAEA Fusion Energy Conference, Daejeon, Republic of Korea (2010)).*

Preprint of Paper to be submitted for publication in Proceedings of the
39th European Physical Society Conference on Plasma Physics, Stockholm, Sweden
2nd July 2012 - 6th July 2012

1. INTRODUCTION.

Surface temperature and heat flux measurements are important issues in high power fusion devices to guarantee safe plasma operation. In the JET tokamak, few embedded ThermoCouples (TC) located 1 cm below the tile surface are used to measure the bulk temperatures of the CFC tiles (coated with about 20 mm of tungsten with the ITER-like wall). We propose here to use an inverse thermal calculation based on Quadruple thermal method to locally deduce the surface temperature (thus on the W coating) and deposited heat flux. The calculation requires the position of the peak (provided by offline magnetic reconstruction) and the qualitative 1D-shape of the heat flux deposited on the target (determined with an empirical expression of the target heat load profile found in ASDEX Upgrade and JET).

2. DESCRIPTION OF THE JET EXPERIMENT AND DIAGNOSTIC SET-UP.

The inverse heat flux calculation has been applied to 2.2T/2MA ELMy H-mode Pulse No: 82641 performed with NBI heating (10MW during 4s) and with the high-field and low-field sides strike points on the vertical targets (low triangularity vertical tile configuration, see figure 1-a). The diagnostic set-up is made of InfraRed (IR) thermography system (wide angle equatorial viewing with spatial resolution of ~ 16 mm in the divertor region) to measure the surface temperature and four embedded type-K thermocouples (TC) 10mm below the tile surface to measure the bulk temperatures of the inner and outer vertical target plates (two TCs by tile as shown in figure 1-b, the upper TC is located at $Z_{TC}^U = -1.557$ m and the lower one at $Z_{TC}^L = -1.65$ m from the equatorial mid-plane). For Pulse No: 82641 the inner and outer strike point (ISP/OSP) positions are given by the magnetic equilibrium with typical uncertainties of ± 0.5 cm on the vertical tiles $Z^{ISP} = -1.568$ m (~ 1.2 cm bellow TC3U) and $Z^{OSP} = -1.565$ m (~ 0.8 cm bellow TC7U).

The IR and TC data reported during Pulse No: 82641 are shown in figure 2-a and 2-b respectively. The brightness surface temperature measurement gives about 400°C (during the inter-ELM phase) on the outer tile shown in figure 2-a at the end of the 4s NBI heating phase assuming the emissivity of the W coated tile is constant and equal to 0.4 [1]. In the same time the bulk temperature increases by 100° and 140° on the inner and outer tile respectively (the total heating integrates inter-ELM and ELM phases).

3. INVERSE HEAT FLUX CALCULATION USING TC DATA.

We propose to use an inverse thermal calculation to deduce the local surface temperature (thus on the W coating) and deposited heat flux using TC data taking into account the bi-dimensional effects due to the orthotropic material ($k_y = k_z$ and $k_x \sim k_z/4$) and the non-uniformity of the heat flux in the x-direction (poloidal). The method is the same as already applied with the MkIIIGB CFC divertor: deconvolution of the thermocouple data with the 2D step response of the tile at the thermocouple location [2]. The 2D step response is computed with the thermal quadrupoles (analytical solution of the heat transfer equation solved in Laplace-Fourier space) therefore with no thermal properties

variation with temperature (linear calculation). The geometry of the carbon tile is approximated by a rectangular tile with a total average thickness e of 4cm and a width L of 17.2cm (Fig.1–b). Uncertainties attributed to the main simplification (geometry plus linearity) are numerically evaluated using 2D FEM modeling, the error bar is $\sim 15\%$ in normal plasma condition (when $T < 500^\circ\text{C}$). The calculation requires the position of the peak (given by the offline reconstruction of the magnetic equilibrium) and the 1D-shape of the heat flux deposited on the target (qualitative shape). The target heat load profile is described with an heuristic expression based on the convolution of the Scrape-Off Layer (SOL) exponential profile with a Gaussian width S representing the diffusion of the heat flux toward the targets (resulting from the parallel and perpendicular transport in the divertor) [3]:

$$q(s) = \frac{Q_0}{2} \exp\left(\frac{S}{2\lambda_q f_x}\right)^2 - \frac{\bar{s}}{\lambda_q f_x} \cdot \text{erfc}\left(\frac{S}{2\lambda_q f_x} - \frac{\bar{s}}{S}\right) + Q_{BG} \text{ and } \bar{s} = s - s_0 \quad (1)$$

Where s is the target coordinate, s_0 is the strike line position, f_x is the magnetic flux expansion (integrated from the outer midplane to the target), λ_q is the SOL power decay length and Q_0 is the peak heat load on the strike line position (i.e. the parameter that we propose to deduce with the TC data). The power decay length λ_q is given by an empirical scaling based on IR thermography analysis (mainly performed during JET and AUG C-wall operation):

$$\lambda_q^{JET} = 0.7 \cdot B^{-0.84} (T) \cdot q^{1.23} \cdot P_{SOL}^{0.14} (MW) \cdot P_{geo}^{0.02} (m) \quad (2)$$

Where B is the magnetic field, q is the cylindrical safety factor and P_{SOL} is the power crossing the separatrix ($P_{SOL} = P_{tot} - P_{rad}$). For Pulse No: 82641, $B = 2.2\text{T}$, $q = 3.2$, $P_{SOL} \sim 7\text{MW}$, we find $\lambda_q = 2\text{mm}$. The vertical outer target heat load profile given by (1) is shown in figure 3 for Pulse No: 82641, $f_x = 8$, $\lambda_q = 2\text{mm}$, full line $S = 1\text{mm}$ ($S/\lambda_q = 0.5$, mean value of the JET data) and dashed line $S = 2\text{mm}$ ($S/\lambda_q = 1$, maximum value of the JET data). The inverse heat flux calculation has been applied with the 1D-shape presented above ($\lambda_q = 2\text{mm}$, $S = 1\text{mm}$, $f_x = 8$ and $Q_{BG} = 100\text{kW/m}^2$ attributed to plasma radiation). Peak heat loads are found to be $Q^{ISP} = 3\text{MW/m}^2$ and $Q^{OSP} = 5\text{MW/m}^2$ with $\pm 15\%$ uncertainties at the Inner Strike Point (ISP) and Outer Strike Point (OSP). The corresponding surface temperatures and total accumulated energy (output power integrated over the pulse) are of $400^\circ\text{C}/12\text{MJ}$ (OSP) and $280^\circ\text{C}/5.6\text{MJ}$ (ISP) at the end of the heating phase (lasting 4s). The surface temperature target profiles derived from TC data (QUAD calculation) and IR images (using an emissivity of W of 0.4 [1]) are compared in figure 4–b. A relatively good agreement is obtained near the strike point (typically when $T > 300^\circ\text{C}$) while a strong discrepancy is observed on the rest of the target (when temperature are below 300°). Further investigation would be required to understand the discrepancy at low temperatures (taking into account emissivity and reflection issues for IR data and strike point positioning and I_q uncertainties with the inverse TC calculation).

CONCLUSIONS.

The combination of the inter-ELM empirical target heat load profile proposed in [3] (limited to attached plasmas) with an inverse heat flux calculation using embedded TC data provides a new way to compute heat load and surface temperature on targets (integrating inter-ELM and ELM phases). The first application to JET data with the ILW shows satisfactory results (temperature, heat load and energy). The main advantage of the method is that it is independent of surface layers, emissivity and reflection issues (associated to IR thermography in metal environment) while its main disadvantages are the poor spatial covering (due to the low number of TC present in the machine) in one side and the strike point position uncertainty (of the order of $\text{cm} \gg \lambda_q$) in the other side. In metallic wall environment IR thermography and embedded TC are two complementary systems to guarantee the accuracy of the temperature and heat load measurements.

ACKNOWLEDGEMENTS

This work was supported by EURATOM and carried out within the framework of the European Fusion Development Agreement. The views and opinions expressed herein do not necessarily reflect those of the European Commission.

REFERENCES

- [1]. S. Devaux et al. Submitted to Journal of Nuclear Materials 2012
- [2]. J.-L. Gardarein et al. International Journal of Thermal Science, **48** (2009) 1-13
- [3]. T. Eich et al., Physical Review Letters **107** (2011) 215001

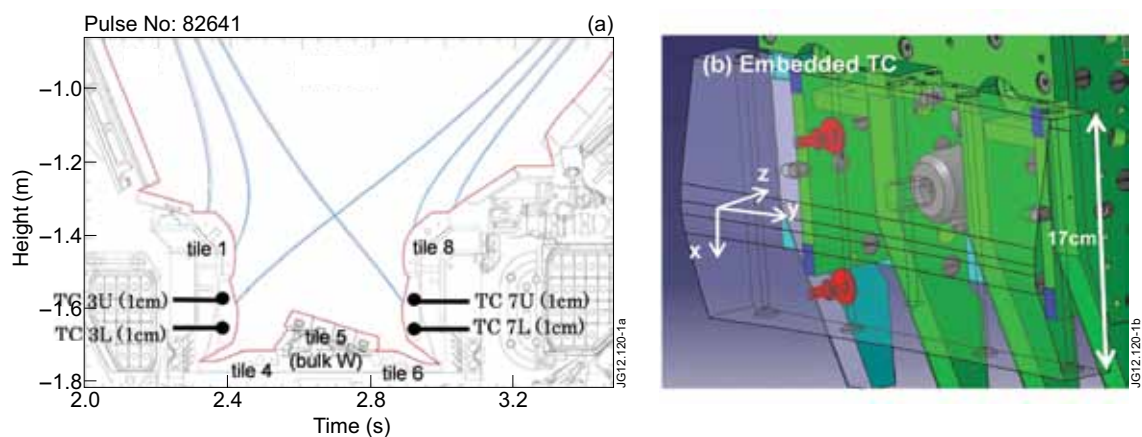


Figure 1: (a) Poloidal cross-section of the divertor with the magnetic equilibrium and position of the TCs in the inner and outer targets. (b) View of the outer vertical tile with upper and lower embedded TCs.

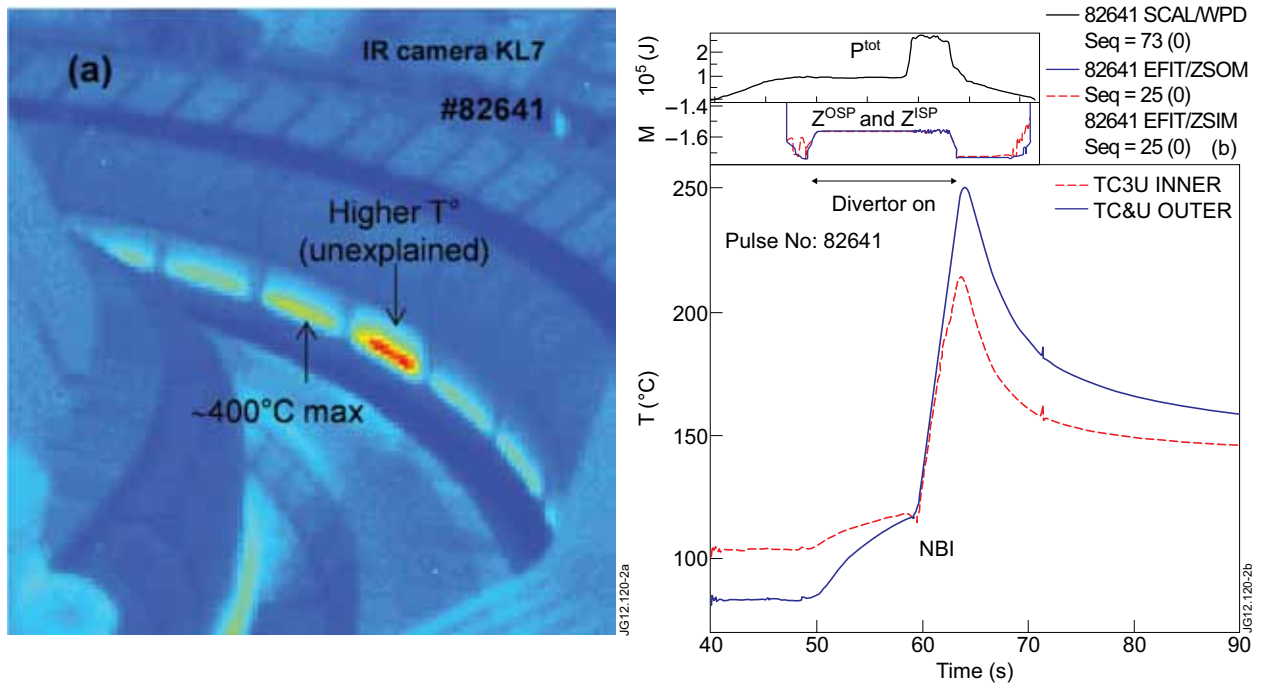


Figure 2: (a) IR data ($t = 23s$) taken from the wide angle viewing camera (KL7 IR camera) during Pulse No: 82641. (b) Inner (TC3U, red curve) and outer (TC7U, blue curve) TC data during Pulse No: 82641.

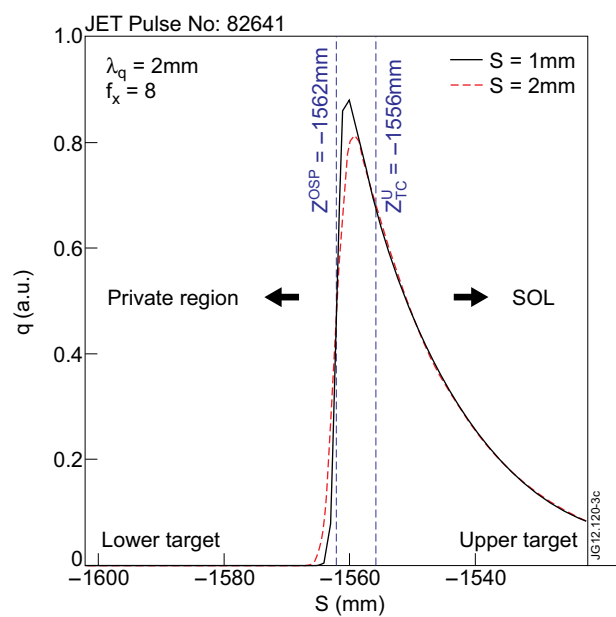


Figure 3: Normalized target heat load profile on the outer vertical tile for $S = 1mm$ and $S = 2mm$.

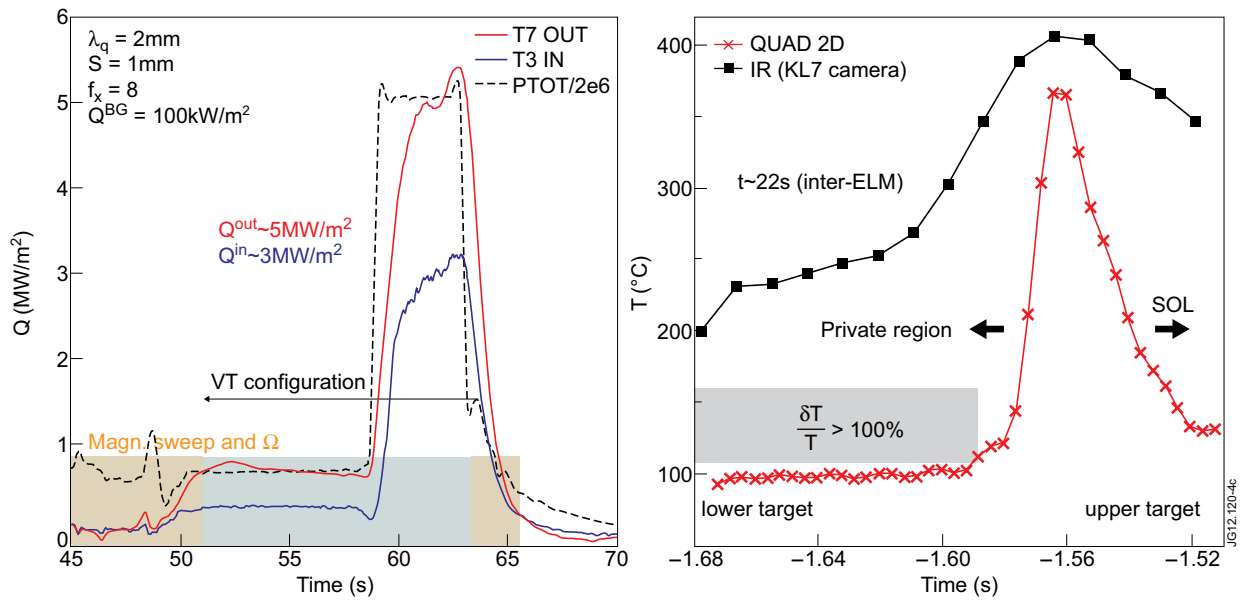


Figure 4: (a) Inner / outer heat load computed with the 2D-QUAD method. (b) Surface temperature profiles along the OUTER vertical tile measured with TC (crosses) and wide angle IR (squares).